© 2014. Published by The Company of Biologists Ltd | Journal of Cell Science (2014) 127, 4870–4882 doi:10.1242/jcs.152231

RESEARCH ARTICLE

rpS6 regulates blood–testis barrier dynamics through Akt-mediated effects on MMP-9

Ka-Wai Mok, Dolores D. Mruk and C. Yan Cheng*

ABSTRACT

Mammalian target of rapamycin complex 1 (mTORC1) is an emerging regulator of blood–tissue barriers that utilizes ribosomal protein S6 (rpS6) as the downstream signaling molecule. To explore the role of rpS6 in blood–testis barrier (BTB) function, a constitutively active quadruple rpS6 phosphomimetic mutant was constructed in mammalian expression vector and overexpressed in Sertoli cells cultured *in vitro* that mimicked the BTB *in vivo*. Using this quadruple phosphomimetic mutant, phosphorylated (p)-rpS6 was shown to disrupt IGF-1/insulin signaling, thereby abolishing Akt phosphorylation, which led to an induction of MMP-9. This increase in MMP-9 secretion perturbed the Sertoli cell tight junction permeability barrier by proteolysis-mediated downregulation of tight junction proteins at the BTB. These findings were confirmed by the use of a specific MMP-9 inhibitor that blocked the disruption of the tight junction permeability barrier by the rpS6 mutant. Additionally, RNA interference (RNAi)-mediated Akt silencing was able to mimic the results of rpS6 mutant overexpression in Sertoli cells, further confirming this p-rpS6–Akt–MMP-9 signaling pathway. In conclusion, these data support a new concept of mTORC1-mediated BTB regulation, that is possibly also applicable to other blood–tissue barriers.

KEY WORDS: Testis, rpS6, Blood–testis barrier, Spermatogenesis, Seminiferous epithelial cycle, Sertoli cells, Germ cell transport, F-actin, Ectoplasmic specialization, Tight junction

INTRODUCTION

In the mammalian testis, tight junctions, basal ectoplasmic specializations (a testis-specific adherens junction), gap junctions and desmosomes between adjacent Sertoli cells create the blood–testis barrier (BTB), which divides the seminiferous epithelium into the basal and the apical compartments (Cheng and Mruk, 2012). The BTB is one of the tightest blood–tissue barriers, formed by arrays of F-actin uniquely packed as microfilament bundles sandwiched between the plasma membrane and cisternae of the endoplasmic reticulum of the Sertoli cells, an arrangement that is not seen in other blood–tissue barriers (Cheng and Mruk, 2012; Mruk et al., 2008). These tightly packed F-actin bundles also serve as attachment sites for the tight junction, basal ectoplasmic specialization and gap junction proteins, thus conferring the remarkable features of the BTB (Cheng and Mruk, 2010; Cheng and Mruk, 2012). Despite its tightness, the BTB undergoes cyclic restructuring during spermatogenesis so that preleptotene spermatocytes are transported across the BTB at stage VII–VIII of the epithelial cycle to enter the apical compartment for maturation (Cheng and Mruk, 2010; Cheng and Mruk, 2012; Smith and Braun, 2012). Although these morphological cellular events were described in detail several decades ago (Russell, 1977), the mechanism(s) by which the tight junction and basal ectoplasmic specialization proteins are being reorganized to facilitate this process remains unknown.

Mammalian target of rapamycin complex 1 (mTORC1) is regarded as the main switch of protein synthesis (Laplante and Sabatini, 2012). However, recent studies reveal that mTORC1 signaling is also responsible for a variety of cellular events (Weichhart, 2012), including barrier function modulation (Mok et al., 2013a). Interestingly, at the BTB, mTORC1 was shown to regulate the tight junction barrier through a downstream molecule called ribosomal protein S6 (rpS6), a subunit of eukaryotic ribosomes that is involved in the regulation of protein synthesis (Meyuhas, 2008). For instance, knockdown of rpS6 has been found to tighten the tight junction permeability barrier formed by primary cultured Sertoli cells, through the induction of tight junction proteins (Mok et al., 2012). This suggests that phosphorylated (p)-rpS6 is involved in BTB restructuring by regulating the steady-state levels of tight junction proteins by a yet-to-be-defined mechanism (Mok et al., 2012). We hypothesized that p-rpS6 in mTORC1 signaling perturbed the Sertoli cell tight junction barrier by increasing the level of secreted matrix metalloproteinase-9 (MMP-9), consequently downregulating tight junction proteins at the Sertoli cell–cell interface. We also postulated that the induction of MMP-9 by p-rpS6 was mediated by the downregulation of p-Akt following attenuation of insulin/insulin-like growth factor 1 (IGF-1) signaling. The following studies were performed to test this hypothesis.

RESULTS

Spatiotemporal expression of p-rpS6-Ser235, -Ser236, -Ser240 and -Ser244 coincides with BTB restructuring during the epithelial cycle

An earlier report identified p-rpS6 as the effector of mTORC1 signaling in regulating BTB, but this report focused only on phosphorylation at Ser235 and Ser236 (Mok et al., 2012). We extended this earlier study to include the phosphorylation sites at Ser240 and Ser244, by first investigating their stage-specific localization in the epithelium during the epithelial cycle (Fig. 1A,B; supplementary material Table S1). Although total rpS6 was present at the BTB at all stages without displaying stage specificity (Mok et al., 2012), rpS6 phosphorylated at Ser235 and Ser236, as well as that phosphorylated at Ser240 and Ser244 was expressed at the BTB during stages VIII–IX, coinciding with the

The Mary M. Wohlford Laboratory for Male Contraceptive Research, Center for Biomedical Research, Population Council, 1230 York Avenue, New York, NY 10065, USA.

*Author for correspondence (Y-Cheng@popcbr.rockefeller.edu; ccheng@rockefeller.edu)

Received 25 February 2014; Accepted 1 September 2014

Journal of Cell Science

Journal of Cell Science (2014) 127, 4870–4882 doi:10.1242/jcs.152231

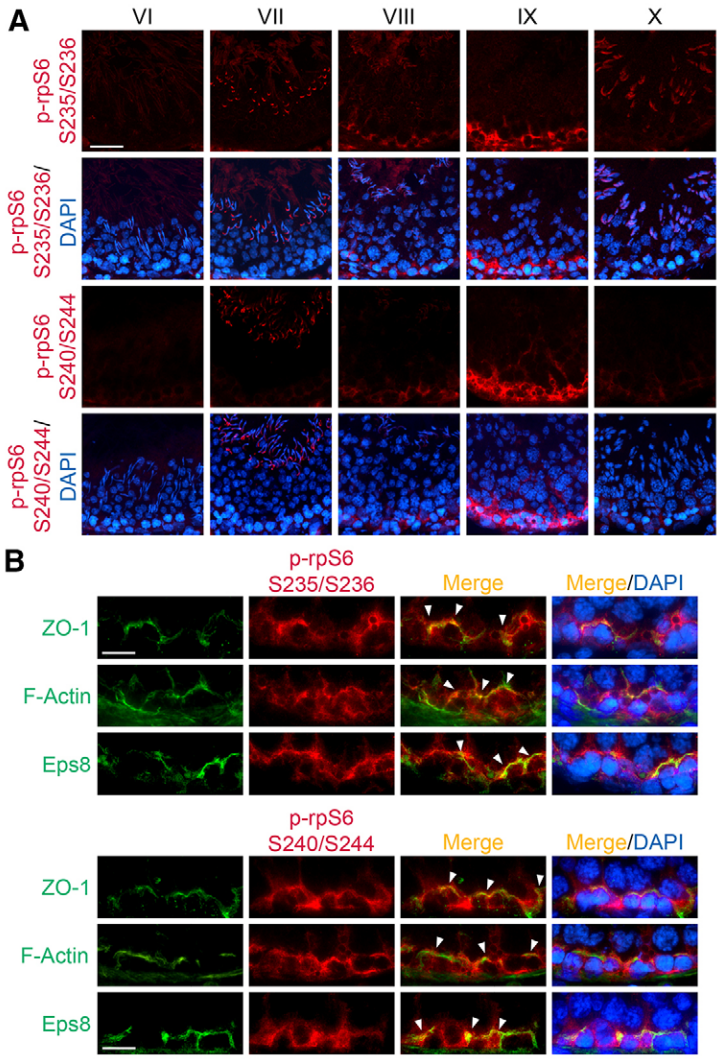

Fig. 1. Stage-specific localization of p-rpS6-Ser235/236 and p-rpS6-Ser240/244 at the BTB in the seminiferous epithelium of adult rat testes. (A) Using immunofluorescence microscopy of frozen sections, the localization of p-rpS6-Ser235/236 (red) and p-rpS6-Ser240/244 (red) in the seminiferous epithelium was examined. These proteins were found to show stage-specific localization at the BTB. (B) These proteins colocalized with the BTB proteins ZO-1 (green), actin (green) and Eps8 (green) (white arrowheads) in late stage VIII or IX. Nuclei were stained with DAPI (blue). It was noted that the phosphorylated proteins first appeared at the BTB during stage VIII, were more robust during stage IX, but diminished considerably and became barely detectable during stage X. Scale bars: 50 μm (A) and 25 μm (B).

time of BTB restructuring to facilitate the transport of preleptotene spermatocytes across the barrier (Fig. 1A). Partial colocalization of p-rpS6 with several putative BTB proteins at stage IX are shown in Fig. 1B, confirming the localization of p-rpS6 at the BTB. Given this timely activation of rpS6, it was postulated that the phosphorylation of these four sites of rpS6 might be necessary to facilitate BTB restructuring.

Overexpression of wild-type rpS6 or an rpS6 quadruple phosphomimetic mutant perturbs the tight junction permeability barrier *in vitro* by the induction of MMP-9 activity

Overexpression of p-rpS6 in Sertoli cells induces tight junction permeability barrier disruption

In order to further investigate the involvement of p-rpS6 in BTB restructuring, we used site-directed mutagenesis to prepare an rpS6 quadruple phosphomimetic mutant in which Ser235, Ser236, Ser240 and Ser244 residues were replaced by glutamic acids (Vallejo et al., 2008). This mutant was therefore constitutively active and is referred to here as active rpS6. An *in vitro* primary cultured Sertoli cell model was employed for the overexpression of this mutant. The wild-type rpS6 as well as the empty vector served as controls, allowing us to investigate the effects of p-rpS6 on the BTB. It should be noted that these primary cultured Sertoli cells establish a functional tight junction barrier, with tight junctions, basal ectoplasmic specializations, gap junctions and desmosomes, thus mimicking the *in vivo* Sertoli cell BTB (Lee and Cheng, 2003; Siu et al., 2005). This *in vitro* system is widely used by investigators to study BTB dynamics (Janecki et al., 1992; Lie et al., 2012; Nicholls et al., 2009; Qiu et al., 2013). Furthermore, findings obtained by using this *in vitro* system have been reproduced in studies *in vivo* (Lui et al., 2003; Qiu et al., 2013; Su et al., 2012; Wan et al., 2013), illustrating its physiological relevance. As such, the effect of p-rpS6 on the Sertoli cell tight junction barrier was first investigated by quantifying changes in the tight junction permeability across the Sertoli cell epithelium following the overexpression of different constructs. Overexpression of wild-type rpS6 per se perturbed the tight junction barrier when compared with overexpression of the empty vector (Fig. 2A); however, further disruption was induced by active rpS6 (Fig. 2A). Overexpression of wild-type or active rpS6 led to a ~40% increase in the amount of total rpS6 protein versus empty vector (Fig. 2B; supplementary material Fig. S1). Expression of wild-type rpS6 also upregulated p-rpS6 (Fig. 2B; supplementary material Fig. S1), probably owing to the fact that more rpS6 protein was available as a substrate for the relevant kinases (the S6Ks). Surprisingly, overexpressing active rpS6 caused a further increase in p-rpS6 (Fig. 2B; supplementary material Fig. S1). This increase in

Journal of Cell Science (2014) 127, 4870–4882 doi:10.1242/jcs.152231

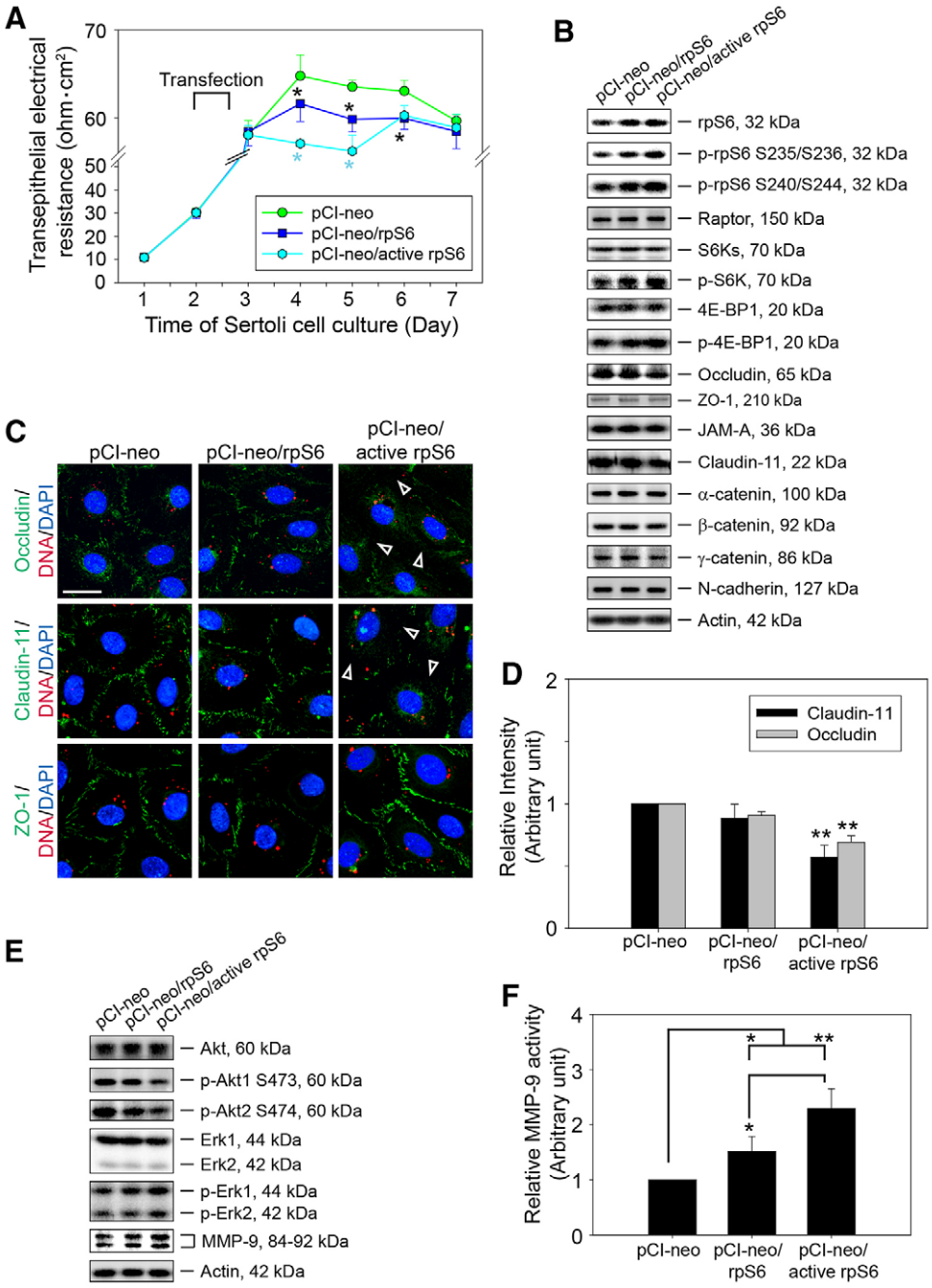

Fig. 2. See next page for legend.

p-rpS6 (shown in Fig. 2B) did not correspond to the rpS6 phosphomimetic mutant following its overexpression in Sertoli cells, because the mutant would not be recognized by the phosphospecific antibodies. Moreover, the expression of active rpS6 versus empty vector induced an approximately twofold increase in the phosphorylation of the two substrates of mTORC1, namely S6Ks and 4E-BP1 (Shah et al., 2000) (Fig. 2B; supplementary material Fig. S1). Thus, these findings suggest that p-rpS6 might enhance the mTORC1 activity by a yet-to-be-defined mechanism. The activated S6Ks would, in turn, phosphorylate more rpS6, forming a positive-feedback loop. This possibility is supported by the surge in p-rpS6 expression at the BTB from stage VII to stages VIII–IX of the epithelial cycle (Fig. 1A). Apart from this, overexpressing active rpS6 was found to downregulate the tight junction proteins occludin and claudin-11 when compared with cells transfected with empty vector (Fig. 2B; supplementary material Fig. S1). This finding thus explained why active rpS6 induced a more severe tight junction barrier disruption compared with that induced by wild-type rpS6 (Fig. 2A). In addition, occludin and claudin-11 staining in these cells showed that these two tight junction proteins were considerably reduced at the Sertoli cell–cell interface following overexpression of active rpS6, but not wild-type rpS6 (Fig. 2C,D), thus confirming the immunoblotting data shown in Fig. 2B.

Fig. 2. Overexpression of wild-type or constitutively active quadruple phosphomimetic rpS6 in Sertoli cells perturbs the tight junction permeability barrier *in vitro* by induction of MMP-9. (A) On day 2, Sertoli cells with a functional tight junction barrier were transfected with empty vector (pCI-neo), wild-type rpS6 construct or active rpS6 construct for 18 h. TER across the Sertoli cell epithelium (a measure of tight junction permeability) was monitored each day throughout the experimental period. A drop in TER illustrates a perturbation of tight junction function after transfection with either wild-type or active rpS6. Data show the mean±s.d. (n=4 replicates from a representative experiment, which was repeated three times using different batches of Sertoli cells and yielded similar results); black asterisk, $P<0.05$ (wild-type rpS6 versus empty vector); blue asterisk, $P<0.05$ (active rpS6 versus wild-type rpS6). (B) Immunoblot analysis of rpS6, p-rpS6, raptor, substrates of mTORC1 (such as S6Ks, 4E-BP1 and their corresponding phosphorylated, activated forms) and selected BTB proteins (the tight junction proteins occludin, ZO-1, JAM-A and claudin-11, and the basal ectoplasmic specialization proteins catenins and N-cadherin) in Sertoli cells after the transfection of empty vector, wild-type rpS6 or active rpS6. Cells were harvested on day 4 after performing transfection on day 2. Actin served as a loading control. Data are representative of 4–6 independent experiments using different batches of Sertoli cells (see supplementary material Fig. S1 for composite results of these immunoblots). (C) Changes in the localization of tight junction proteins occludin (green), claudin-11 (green) and ZO-1 (green) at the Sertoli cell–cell interface were examined on day 4, after transfection of different Cy3-labeled plasmid DNAs (red) on day 2. Nuclei were stained with DAPI (blue). After overexpression of active rpS6, changes in the localization of tight junction proteins were noted, and these were quantified in D. Considerably less occludin and claudin-11 were detected at the cell–cell interface (arrowheads) versus cells transfected with pCI-neo vector alone. Scale bar: 50 µm. (D) To quantify changes in the localization of tight junction proteins, the intensities of fluorescent signals of corresponding tight junction proteins were obtained by using ImageJ. Data show the mean±s.d. (n=3 independent experiments with ~50 randomly selected Sertoli cells in each experiment); $^{**}P<0.01$. (E) Immunoblot analysis of selected regulatory proteins including Akt and its two phosphorylated forms, Erk1/2 and their phosphorylated forms, as well as MMP-9 in Sertoli cells after transfection of empty vector, wild-type rpS6 or active rpS6. Data are representative of 4–6 independent experiments, composite data are shown in supplementary material Fig. S1. (F) The amount of secreted MMP-9 in the medium of Sertoli cells transfected with different plasmid DNAs was quantified by using an intrinsic MMP-9 activity assay (see Materials and Methods). The relative MMP-9 activity in pCI-neo (control) was arbitrarily set as 1. Data show the mean±s.d. (n=4 independent experiments); $^{*}P<0.05$; $^{**}P<0.01$.

p-rpS6-induced MMP-9 upregulation is mediated by Akt and Erk

Following overexpression of wild-type and active rpS6 versus empty vector in Sertoli cells with an established functional tight junction barrier, it was noted that although total levels of Akt protein (including Akt1 and Akt2) remained unchanged, the expression of p-Akt1-Ser473 and p-Akt2-Ser474 in cells transfected with wild-type and active rpS6 dropped by ~30% and ~50–70%, respectively (Fig. 2E; supplementary material Fig. S1). This p-rpS6-induced downregulation of p-Akt could account for the induction of p-Erk1/2 (Fig. 2E; supplementary material Fig. S1), as earlier studies have shown that Akt inactivates the Raf–MER–Erk signaling pathway by phosphorylating Raf (Moelling et al., 2002; Zimmermann and Moelling, 1999). This increase in p-Erk1/2 likely induced the expression and activity of MMP-9 (Fig. 2E,F; supplementary material Fig. S1), because MMP-9 expression has been shown to be dependent on the activity of Erk1/2 (Tseng et al., 2013; Tyagi et al., 2009). To test the hypothesis that Erk1/2 activation is required for p-rpS6-induced MMP-9 upregulation, a specific Erk1/2 inhibitor (U0126) was used. U0126 treatment was able to fully abolish Erk1/2 phosphorylation, even in Sertoli cells overexpressing wild-type or active rpS6, which could have induced Erk1/2 activation (supplementary material Fig. S2A,B). It was noted that after treating Sertoli cells with U0126, the phosphorylation of rpS6 was prevented in cells transfected with empty vector, wild-type rpS6 or active rpS6 compared with that observed in untreated cells transfected with empty vector (supplementary material Fig. S2A,B), consistent with earlier reports illustrating that Erk1/2 is indispensable in mediating the activation of mTORC1 (Ma et al., 2005; Roux et al., 2004). The level of total rpS6 was also found to be downregulated in all U0126-treated cells (supplementary material Fig. S2A,B). An earlier study has reported that blockade of Erk1/2 activation attenuates the upregulation of total rpS6 protein level induced by long-term potentiation (LTP) in rat hippocampus (Tsokas et al., 2007). Although the basal level of rpS6 was reduced by ~15% compared with that of controls following U0126 treatment in this previous report (Tsokas et al., 2007), we found that rpS6 expression was considerably reduced by ~40–60% in Sertoli cells (supplementary material Fig. S2A,B) in our experiments as reported herein. This difference could be accounted for by a longer treatment time; a 48-h incubation was performed here (because we elected to block the constitutively active rpS6 following overexpression) versus a 1-h pretreatment. More importantly, the induction of MMP-9 after overexpression of wild-type or active rpS6 was blocked by U0126-mediated Erk1/2 inhibition (supplementary material Fig. S2A), confirming the role of Erk1/2 in MMP-9 stimulation. Furthermore, as MMP-9 was not induced, the downregulation of the tight junction protein occludin that was caused by active rpS6 was also abolished (supplementary material Fig. S2A). Interestingly, another tight junction integral membrane protein, claudin-11, was found to be upregulated by almost sevenfold in U0126-treated cells in different regimens (supplementary material Fig. S2A,B). This observation is consistent with earlier findings that the activation of Erk1/2 is involved in the disruption of the epithelial tight junction barrier by downregulating tight junction proteins (Petecchia et al., 2012; Samak et al., 2011). Collectively, these data support the notion that overexpression of wild-type or active rpS6 leads to a downregulation of p-Akt, resulting in the activation of Raf–MER–Erk signaling that upregulates MMP-9. This idea is also supported by an earlier study demonstrating that MMP-9 is induced after p-Akt is downregulated following the disruption of mTORC2 signaling [mTORC2 is responsible for phosphorylating Akt1 at Ser473 and Akt2 at Ser474 (Dillon and Muller, 2010)] by silencing rictor (Das et al., 2011), the key binding partner of mTORC2 (Oh and Jacinto, 2011).

p-rpS6-induced BTB disruption is mediated by MMP-9

MMP-9 is a secretory protease; however, it is synthesized and secreted as a latent inactive pro-enzyme, which is then activated by cleavage (Björklund and Koivunen, 2005) to generate an active protease, at or near the Sertoli cell surface, by a process involving membrane-type 1 (MT1)-MMP and tissue inhibitor of metalloproteases-2 (TIMP2) (Longin et al., 2001; Siu and Cheng, 2004). Herein, we sought to determine whether activated MMP-9 was indeed induced by quantifying the amount of active MMP-9 in the Sertoli cell culture medium following overexpression of rpS6 and its mutant. The results showed that overexpression of wild-type rpS6 and active rpS6 caused a ~50% and ~100% increase in active MMP-9 in the medium, respectively (Fig. 2F). Given that the overexpression of active rpS6 induced more p-rpS6 when compared with cells overexpressing wild-type rpS6, these results suggest that p-rpS6 is a key player in MMP-9 induction.

Journal of Cell Science (2014) 127, 4870–4882 doi:10.1242/jcs.152231

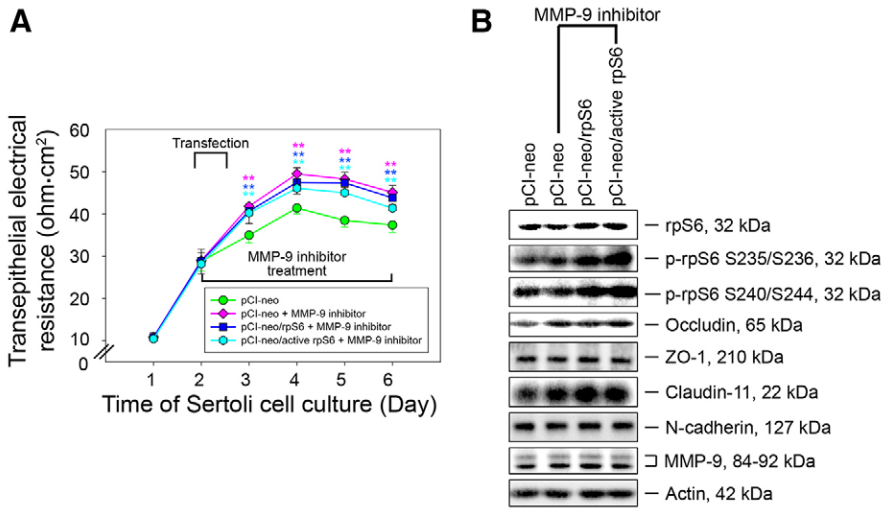

Fig. 3. Inhibition of MMP-9 blocks the disruption of the tight junction permeability barrier caused by wild-type or phosphomimetic rpS6. (A) On day 2, Sertoli cells with an established functional tight junction barrier were transfected with empty vector (pCI-neo), wild-type rpS6 construct (pCI-neo/rpS6) or constitutively active rpS6 quadruple phosphomimetic mutant construct (pCI-neo/active rpS6) in the presence of MMP-9 inhibitor I (5 μM) for 18 h. The inhibitor was included in the replacement F12/DMEM when the media were replaced daily. TER across the Sertoli cell epithelium was recorded daily. An increase in TER illustrated a tightening of the tight junction barrier in the presence of MMP-9 inhibitor I, regardless of the overexpression of the wild-type or constitutively active rpS6, which was shown to induce disruption of the tight junction barrier (see Fig. 2A). Data show the mean±s.d. (n=4 replicates from a representative experiment, which was repeated three times using different batches of Sertoli cells, yielding similar results); $^{**}P<0.01$ (versus pCI-neo alone without MMP-9 inhibitor treatment). (B) Immunoblot analysis of rpS6, p-rpS6, selected tight junction proteins (occludin, ZO-1 and claudin-11), the basal ectoplasmic specialization protein N-cadherin and MMP-9 in Sertoli cells after the transfection of empty vector and in cells treated with MMP-9 inhibitor I (5 μM) and transfected with empty vector, wild-type rpS6 or active rpS6. Cells were harvested on day 4 after performing transfection on day 2. Actin served as a loading control. Data are representative of four independent experiments using different batches of Sertoli cells (see supplementary material Fig. S3A for composite results of these immunoblots).

As MMP-9 was shown to perturb various tissue barriers, including the blood-brain barrier (Chen et al., 2013) and brain–cerebrospinal-fluid barrier (Chiu and Lai, 2013), probably by the degradation of tight junction proteins such as occludin and claudin (Chen et al., 2009; Chiu and Lai, 2013), the induction of MMP-9 by active rpS6 thus explains the observation that active rpS6 caused further disruption of the tight junction barrier compared with wild-type rpS6 (Fig. 2A). To test the hypothesis that MMP-9 is the downstream effector of p-rpS6-mediated BTB restructuring, a specific MMP-9 inhibitor was used to examine whether MMP-9 inhibition could block the active-rpS6-induced disruption of the tight junction barrier. Consistent with our hypothesis, following MMP-9 inhibition, the barrier was considerably tightened (Fig. 3A; supplementary material Fig. S3A), regardless of whether wild-type or active rpS6 was overexpressed (Fig. 3B; supplementary material Fig. S3A). This result confirmed the involvement of MMP-9 in p-rpS6-induced BTB restructuring. This tightening of the tight junction barrier was likely to have been mediated by the induction of tight junction proteins such as occludin and claudin-11 (Fig. 3B; supplementary material Fig. S3A), which could be the result of reduced proteolytic protein degradation following MMP-9 inhibition. Interestingly, the steady-state level of MMP-9 was upregulated following MMP-9 inhibitor treatment (Fig. 3B; supplementary material Fig. S3A), which might be a physiological response of the Sertoli cells in the presence of MMP-9 inhibitor, in an attempt to maintain BTB homeostatic functions, such as junction remodeling. In addition, our hypothesis that p-rpS6 downregulates p-Akt, which leads to an induction of MMP-9 to facilitate BTB restructuring is supported by the stage-specific localization of p-Akt and MMP-9 at the BTB (Fig. 4A,B; supplementary material Fig. S3B,C). The results showed that at stages VIII–IX when p-rpS6 was robustly expressed at the BTB (Fig. 1A), the levels of p-Akt1-Ser473 (Fig. 4A) and p-Akt2-Ser474 (supplementary material Fig. S3B) at the BTB were downregulated versus those observed at stages V–VII. Coinciding with the reduced expression of p-Akt at the BTB in stages VIII–IX tubules, intensive staining of MMP-9 was found at the BTB at these stages (Fig. 4A). Such a reciprocal pattern of expression of p-rpS6, p-Akt and MMP-9 at the BTB in these stages in the testis thus supports the notion that the p-rpS6-dependent induction of MMP-9 is mediated by the downregulation of p-Akt. Furthermore, localization of p-Akt1-Ser473, p-Akt2-Ser474 and MMP-9 at the BTB was confirmed by their colocalization with several BTB-associated proteins (Fig. 4B; supplementary material Fig. S3C).

p-rpS6-dependent regulation of BTB dynamics is mediated by the upstream IGF-1/insulin signaling pathway

p-rpS6 downregulates p-Akt through the disruption of IGF-1/insulin signaling

Although we showed that p-rpS6 downregulates Akt phosphorylation, the underlying mechanism(s) remained unclear. Given that Akt is a substrate of mTORC2 (Sarbassov et al., 2005), we sought to investigate whether the mTORC2 signaling was perturbed. Our results showed that the phosphorylation of other mTORC2 substrates, namely PKC-α and SGK1 (Mok et al., 2013a), and the level of p-mTOR-Ser2481, which is proportional to the amount of mTORC2 (Copp et al., 2009), remained unchanged following the overexpression of wild-type or active rpS6 (Fig. 5A), indicating that mTORC2 signaling was not affected. Note that prior to the phosphorylation of Akt at Ser473 by mTORC2, it has to be

Journal of Cell Science (2014) 127, 4870–4882 doi:10.1242/jcs.152231

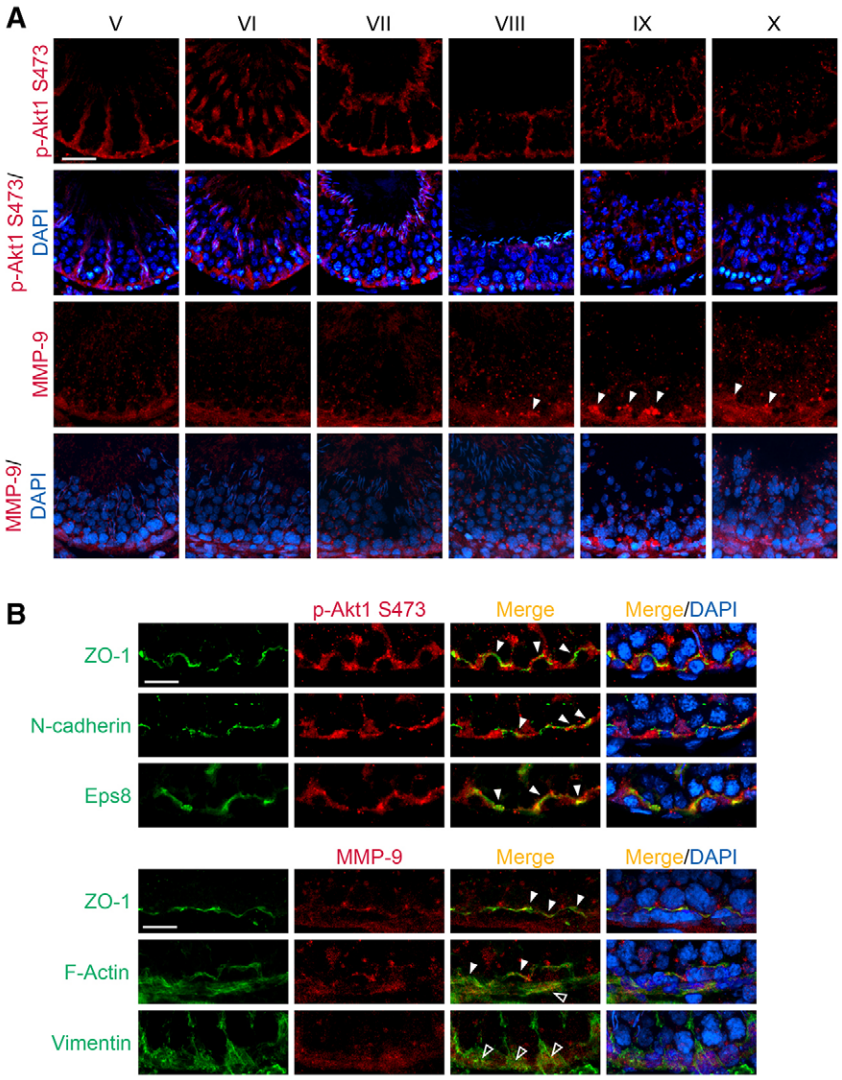

Fig. 4. Stage-specific localization of p-Akt1-Ser473 and MMP-9 at the BTB in the seminiferous epithelium of adult rat testes. Using paraffin-embedded (for Akt) or frozen (for MMP-9) sections of adult rat testes, stage-specific localization of p-Akt1-Ser473 (red) and MMP-9 (red) was shown. (A) Immunofluorescence microscopy demonstrated that p-Akt1-Ser473 was localized in the seminiferous epithelium at the BTB and also localized with apical ectoplasmic specializations, displaying a strict stage-specific pattern of localization at these sites. The amount of p-Akt1-Ser473 at the BTB diminished considerably during stage VIII and it was almost non-detectable at the BTB in stage IX and X. Intense staining of MMP-9 at the BTB was found from stage VIII to stage X and was strongest in stage IX (white arrowheads). Scale bar: 50 μm. (B) p-Akt1-Ser473 was found to colocalize with the BTB proteins ZO-1 (green), N-cadherin (green) and Eps8 (green), and MMP-9 was found to colocalize with the BTB proteins ZO-1 (green), F-actin (green) and vimentin (green) at stages VI–VII. Filled arrowheads indicate proteins colocalized with p-Akt-S473 or MMP-9 at the BTB, near the basement membrane; open arrowheads indicate proteins colocalized with MMP-9 in the peritubular myoid cells, underneath the BTB and the basement membrane. Nuclei were stained with DAPI (blue). See also supplementary material Fig. S3B,C for stage-specific localization of p-Akt2-Ser474 at the BTB in adult rat testes. Scale bars: 25 μm.

first phosphorylated at Thr308, a process dependent on the presence of activated growth factor receptors (Fayard et al., 2010). Moreover, over-activation of mTORC1 signaling has been shown to reduce the levels of p-Akt-Ser473, due to attenuation of growth factor receptor signaling (Harrington et al., 2004; Zhang et al., 2003). Thus, we speculated that p-rpS6, a protein downstream of mTORC1 signaling, would also reduce the levels of p-Akt-Thr308 and, hence, downregulate p-Akt-Ser473. The results showed that among the selected growth factor receptor subunits, the levels of IGF-1R-β and insulin receptor-β were significantly downregulated following the overexpression of wild-type or active rpS6 (Fig. 5B,C), suggesting that the IGF-1/insulin signaling was perturbed. Furthermore, overexpression of active rpS6 significantly reduced p-Akt-Thr308 when compared with the effects of overexpressing wild-type rpS6 (Fig. 5B,D), suggesting that p-rpS6 is the key player in regulating Akt phosphorylation. In order to phosphorylate Akt at Thr308, activated growth factor receptors need to activate phosphatidylinositol 3-kinase (PI3-K) initially, which generates PIP_3 for activating PDK1, which then phosphorylates Akt (Fayard et al., 2010). Thus, an assay to quantify PI3-K activity was performed to confirm the disruption of IGF-1/insulin signaling. The results showed that the intrinsic activity of PI3-K decreased by ∼30% and ∼50% in wild-type- and active-rpS6-overexpressing cells, respectively, versus cells transfected with empty vector (Fig. 5E), confirming the idea that IGF-1/insulin signaling was perturbed. These data support the notion that p-rpS6 disrupts IGF-1/insulin signaling, which reduces p-Akt-Thr308, hence leading to the downregulation of p-Akt-Ser473.

The PI3-K–Akt signaling complex is involved in the IGF-1/insulin signaling pathway upstream, and Erk1/2 is the downstream effector of p-rpS6 signaling

Because a knockdown of rpS6 was able to increase the amount of tight junction protein at the Sertoli cell BTB (Mok et al., 2012), a specific PI3-K inhibitor, LY294002, was used to investigate whether PI3-K inhibition could block the rpS6-mediated effects on the expression of tight junction proteins in Sertoli cells. This thus confirmed the involvement of PI3-K–Akt signaling in p-rpS6-mediated remodeling of the Sertoli cell tight junction barrier. Indeed, LY294002 was shown to block the phosphorylation of Akt (supplementary material Fig. S4A,B), because Akt phosphorylation is a PI3-K–PDK1-dependent process as mentioned above. In addition, it was observed that when Akt phosphorylation was completely abolished, the amount of p-Erk1/2 was considerably increased by as much as sevenfold

Journal of Cell Science (2014) 127, 4870–4882 doi:10.1242/jcs.152231

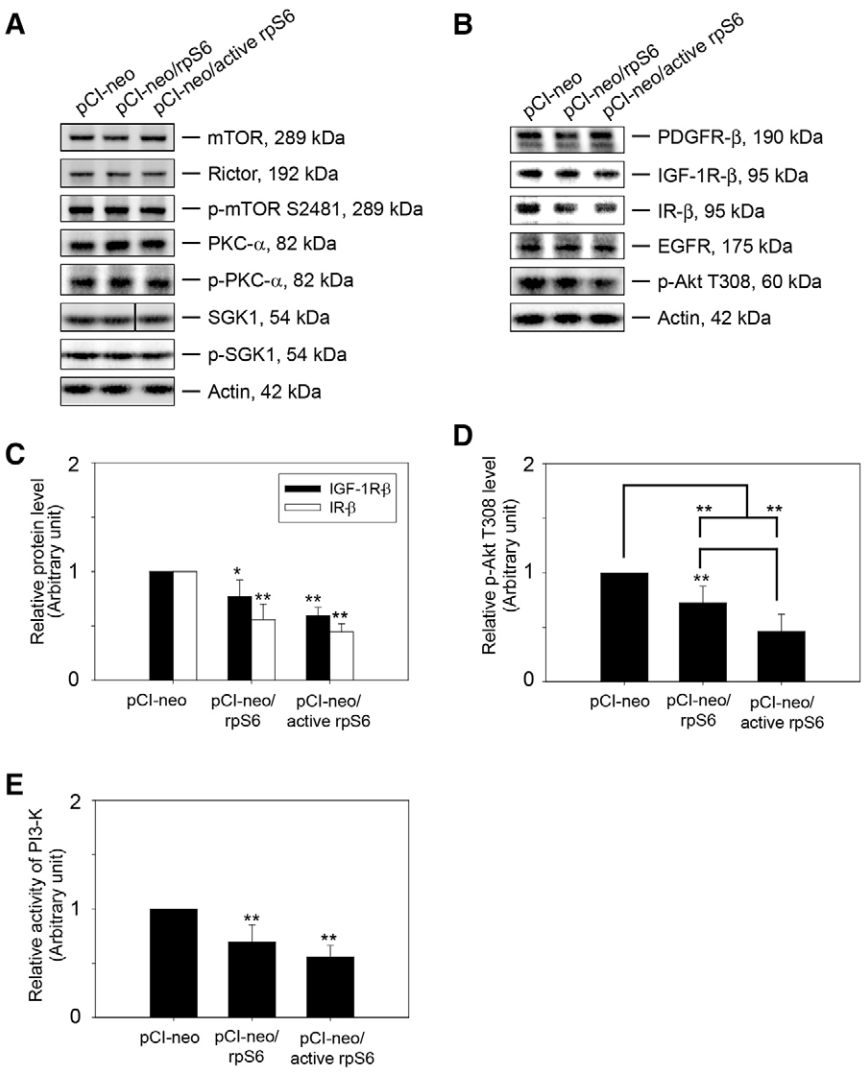

Fig. 5. Reduction in Akt phosphorylation correlates with the disruption of IGF-1/insulin signaling. (A) After transfection of Sertoli cells (which had established a tight junction permeability barrier) on day 2 with empty vector, wild-type rpS6 or constitutively active rpS6 for 18 h, cells were harvested on day 4 and subjected to immunoblotting to quantify the steady-state levels of (1) rictor, which is the key component of mTORC2; (2) p-mTOR-Ser2481, which reflects the integrity of mTORC2; and (3) substrates of mTORC2, including PKC and SGK, and their phosphorylated, activated forms. (B) The levels of selected growth factor subunits, such as IGF-1R-β, IR-β and p-Akt-Thr308, were quantified by immunoblotting to assess whether there was any disruption of IGF-1/insulin signaling. Actin served as the loading control. Data are representative findings of four independent experiments using different batches of Sertoli cells. (C–D) Summary of immunoblotting results shown in A,B. Data represent the mean±s.d. (n=4 experiments). Target proteins that did not show any significant changes were not included. Each data point was normalized against the corresponding actin level and then against the protein level in pCI-neo, which was arbitrarily set at 1. *P<0.05; **P<0.01; versus the pCI-neo control group. (E) A PI3-K activity assay was performed to assess changes in PI3-K intrinsic activity after transfection of Sertoli cells with different vectors. Sertoli cells were harvested on day 4 and lysates were subjected to immunoprecipitation using an anti-PI3-K antibody (Table S1), and PI3-K-containing agarose beads were used for competitive ELISA (see Materials and Methods). The relative PI3-K activity in pCI-neo was arbitrarily set at 1. Data show the mean±s.d. (n=4 experiments); **P<0.01 (versus the pCI-neo control group).

(supplementary material Fig. S4A,B), thus supporting the hypothesis that p-rpS6-induced downregulation of p-Akt would lead to the activation of Erk1/2. More importantly, the results showed that in Sertoli cells that were not treated with LY294002, the knockdown of rpS6 induced p-Akt (supplementary material Fig. 4A,B). This induction of p-Akt could be attributed to a reduction in the amount of p-rpS6 after the knockdown of rpS6 (supplementary material Fig. S4A,B), confirming the findings from the current report showing that p-Akt was downregulated by overexpression of the phosphomimetic p-rpS6 mutant (Fig. 2; supplementary material Fig. S1). The results also indicated that, following LY294002 treatment, phosphorylation of rpS6 was completely abolished (supplementary material Fig. S4A,B), consistent with previous studies demonstrating that PI3-K–Akt signaling is required for activating mTORC1 (Laplante and Sabatini, 2012). Moreover, and consistent with our previous findings (Mok et al., 2012), these data showed that in Sertoli cells that were not treated with LY294002, the knockdown of rpS6 was able to significantly induce the expression of the tight junction protein claudin-11 versus that observed in cells treated with control siRNA, owing to a reduction in the amount of p-rpS6 following rpS6 knockdown (supplementary material Fig. S4A,B). More importantly, after PI3-K inhibition by LY294002, the tight junction proteins occludin and claudin-11 were found to be downregulated (control siRNA or rpS6 siRNA versus corresponding control siRNA or rpS6 siRNA with LY294002 treatment) (supplementary material Fig. S4A,B), and these changes could be the result of an induction of MMP-9 after LY294002 treatment (versus control siRNA) (supplementary material Fig. S4A,B), also involving the activation of Erk1/2 after the inhibition of PI3-K–Akt signaling. This thus supports the hypothesis that the downregulation of tight junction proteins induced by p-rpS6 was mediated by MMP-9 induction as a result of Erk1/2 activation. Collectively, these findings confirm the role of PI3-K–Akt signaling in p-rpS6-mediated disruption of the tight junction barrier by demonstrating the MMP-9-dependent downregulation of tight junction proteins following Erk1/2 activation that was caused by the inhibition of PI3-K–Akt signaling. Furthermore, it is important to note that although the phosphorylation of rpS6 was blocked entirely by PI3-K inhibition, activation of Erk1/2 was still able to induce MMP-9 expression, indicating that Erk1/2 is the downstream effector of p-rpS6 in regulating BTB restructuring.

Journal of Cell Science (2014) 127, 4870–4882 doi:10.1242/jcs.152231

RNAi-mediated knockdown of Akt1 and Akt2 mimics phenotypes resulting from the overexpression of wild-type or active rpS6 at the Sertoli cell BTB

As noted herein, p-rpS6 might induce MMP-9 by downregulation of p-Akt. In order to further confirm the involvement of p-Akt in p-rpS6 signaling, Akt was silenced by RNA interference (RNAi) to assess any changes in the function of the Sertoli cell permeability barrier. Herein, we elected to knock down Akt1 and Akt2, but not Akt3, because Akt1 and Akt2 are ubiquitously expressed in mammalian cells and tissues, whereas Akt3 is expressed mainly in brain, heart and kidney (Masure et al., 1999). Following the knockdown of Akt1 and Akt2 by ~50%, the Sertoli cell tight junction barrier was indeed perturbed (Fig. 6A–C). More importantly, the knockdown of Akt was accompanied by a ~50% drop in both p-Akt1-Ser473 and p-Akt2-Ser474 (Fig. 6B,C). Although the activation of Akt is essential for cell survival – allowing cells to withstand apoptotic stimuli (Song et al., 2005) – the disruption of the Sertoli cell tight junction

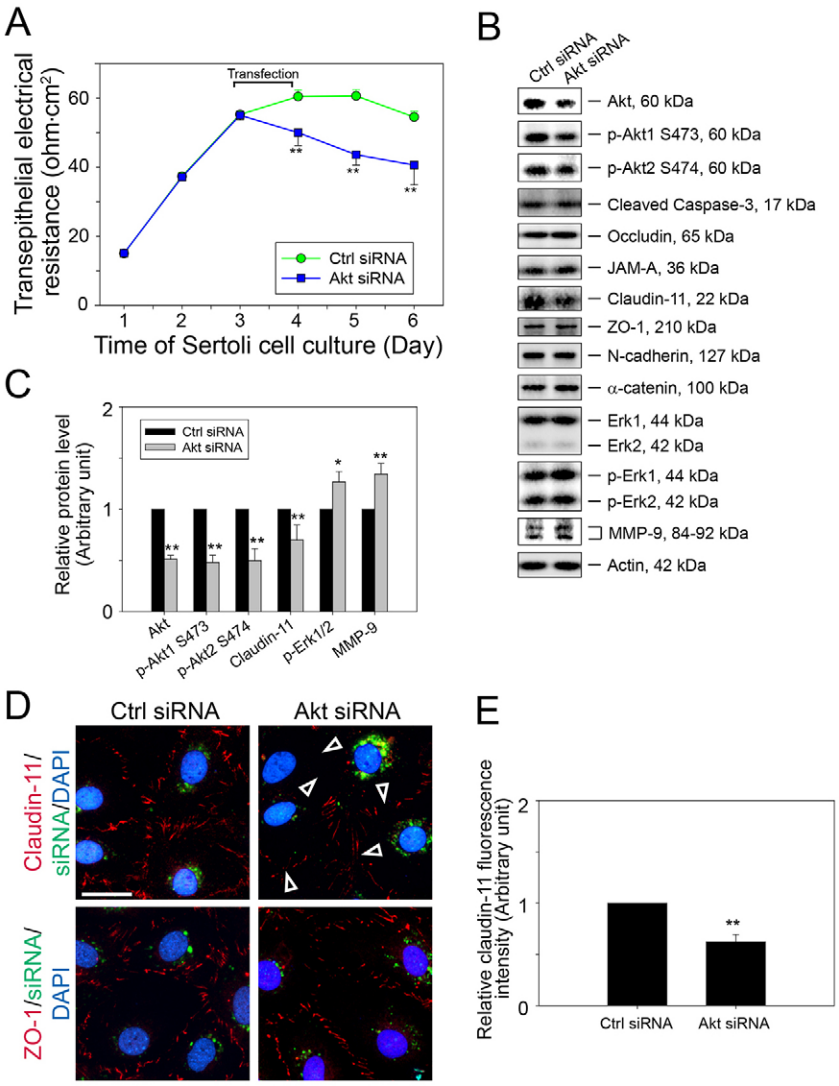

Fig. 6. Akt is the crucial signaling molecule through which rpS6 mediates MMP-9 induction at the Sertoli cell BTB. (A) On day 3, Sertoli cells were transfected with Akt1- and Akt2-specific siRNA duplexes, as well as non-targeting control (Ctrl) siRNA duplexes, for 24 h. Thereafter, changes in the function of the tight junction permeability barrier were assessed. Data show the mean±s.d. (n=4 replicates from a representative experiment, which was repeated three times using different batches of Sertoli cells, yielding similar results); **P<0.01. (B) The effect of Akt1 and Akt2 knockdown by RNAi on selected BTB proteins, such as tight junction proteins (occludin, JAM-A, claudin-11, ZO-1) and basal ectoplasmic specialization proteins (N-cadherin, α-catenin), an apoptotic marker (cleaved caspase-3) and signaling and regulatory proteins (p-Akt1, p-Akt2, Erk1/2, p-Erk1/2, MMP-9) was examined by immunoblotting using lysates from Sertoli cells harvested on day 5. Actin serves as the protein loading control. Data are representative of four independent experiments using different batches of Sertoli cells with similar results. (C) Summary of the immunoblotting results shown in B. Proteins that did not show any significant change are not shown. Each data point was normalized against the corresponding actin level and then against the protein level in the control siRNA sample, which was arbitrarily set at 1. Data show the mean±s.d. (n=4 independent experiments). *P<0.05; **P<0.01. (D) Changes in the localization of claudin-11 (red) and ZO-1 (red) in Sertoli cells on day 5 were examined after cells were transfected on day 3 (for 24 h) with different siRNA duplexes and co-transfected with siGLO (green) to assess transfection efficiency. Nuclei were stained with DAPI (blue). Note that when compared with control, a knockdown of Akt1 and Akt2 in Sertoli cells induced mislocalization of claudin-11, with considerably less claudin-11 at the cell–cell interface (open arrowheads; quantified in E), but ZO-1 distribution was unaffected. Scale bar: 50 µm. (E) To quantify the change in the localization of claudin-11, fluorescent signal of stained tight junction protein claudin-11 was measured. Data show the mean±s.d. (n=3 independent experiments); **P<0.01.

Journal of Cell Science (2014) 127, 4870–4882 doi:10.1242/jcs.152231

barrier and the downregulation of p-Akt that resulted from Akt knockdown were not likely to have been a result of apoptosis. This conclusion was supported by the observation that the level of cleaved caspase-3, which is the activated caspase-3 that induces apoptosis (Thorburn, 2004), did not change after Akt knockdown (Fig. 6B). In addition, the downregulation of claudin-11, an integral membrane protein at the Sertoli cell BTB, was detected (Fig. 6B,C), and this was confirmed by immunofluorescence microscopy showing that the level of claudin-11 was reduced at the cell–cell interface (Fig. 6D,E). This loss of claudin-11 thus destabilized the tight junction barrier. We envisioned that the loss of claudin-11 was likely to have resulted from an induction of MMP-9 caused by activation of ERK1/2 following the loss of p-Akt through a transient RNAi-mediated Akt1/2 knockdown (Fig. 6B,C). In conclusion, these findings illustrate that a loss of p-Akt in Sertoli cells following Akt knockdown could perturb the BTB by inducing MMP-9 that downregulates tight junction proteins, mimicking the results obtained by overexpressing the p-rpS6 quadruple phosphomimetic mutant. We thus conclude that p-rpS6 regulates the BTB through Akt signaling.

DISCUSSION

Although a previous study has shown that mTORC1 signaling regulates BTB dynamics through p-rpS6 (Mok et al., 2012), the underlying mechanism(s) remained unclear. Here, by constructing a constitutively active rpS6 using a quadruple phosphomimetic mutant for its overexpression in primary cultured Sertoli cells with a functional tight junction barrier that mimics the BTB *in vivo*, it was demonstrated that the timely expression of p-rpS6 facilitated BTB restructuring by inducing MMP-9 that led to the downregulation of tight junction proteins, including the localization at the Sertoli cell–cell interface. This increase in the amount of MMP-9 was triggered by the activation of Erk1/2, which was mediated by upstream p-Akt through the disruption of IGF/insulin signaling, as depicted in Fig. 7. This hypothesis is supported by the finding that the inhibition of MMP-9 through the use of a specific inhibitor leads to tightening of the Sertoli cell tight junction permeability barrier. In addition, inhibition of Erk1/2 through the use of specific inhibitor also blocks the induction of MMP-9, whereas inhibition of PI3-K–Akt signaling leads to an induction of MMP-9 through Erk1/2 activation. Collectively, these findings thus unequivocally demonstrate the role of PI3-K–Akt–Erk signaling in the p-rpS6-mediated regulation of BTB dynamics. This concept is also supported by downregulating p-Akt through Akt silencing, which was found to perturb the tight junction barrier, mimicking results from cells transfected with constitutively active quadruple phosphomimetic rpS6 mutant. Thus, it can be concluded that p-rpS6, and hence mTORC1 signaling, regulates BTB dynamics through Akt. This hypothesis is now summarized in the schematic diagram shown in Fig. 7.

Although mTORC1 and mTORC2 have previously been regarded as two distinct pathways, with mTORC1 regulating

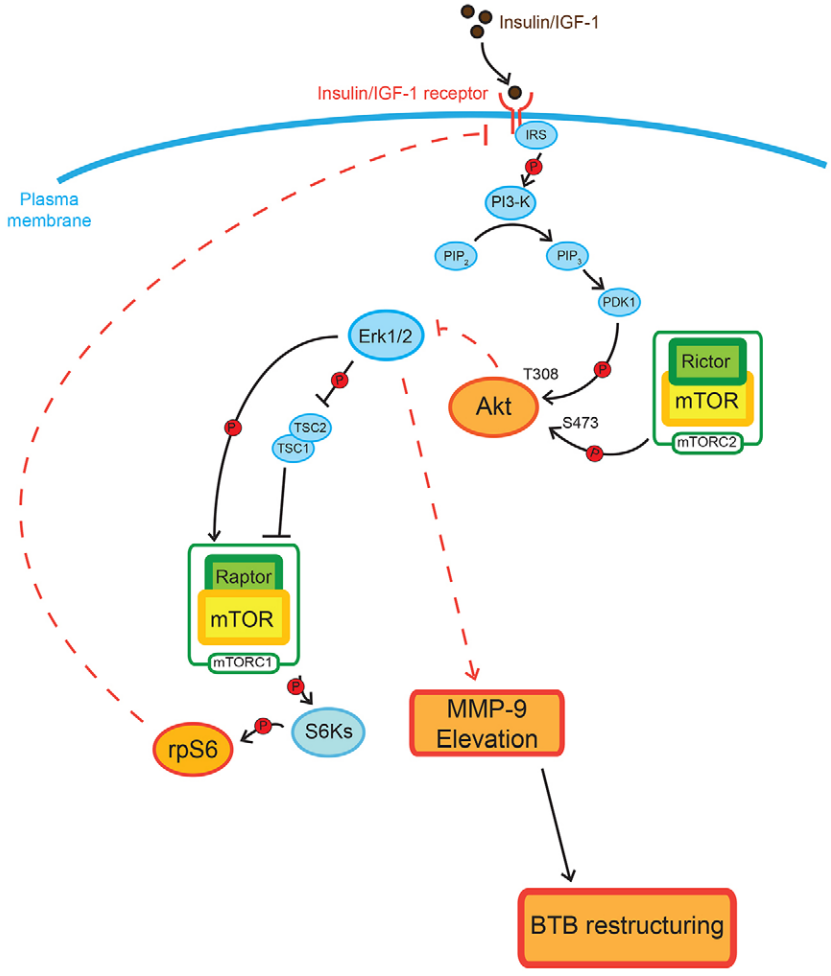

Fig. 7. A proposed mechanism by which rpS6 and mTORC1 signaling regulate BTB dynamics. Activation of rpS6 by S6K-mediated phosphorylation leads to a disruption of IGF-1/insulin signaling. This, in turn, prohibits PI3-K activity and, therefore, phosphorylation of Akt at Thr308 and hence at Ser473 is blocked. Following the removal of the inhibitory effect of p-Akt, activation of ERK 1/2 takes place and this eventually leads to a surge in secreted MMP-9 at the Sertoli cell BTB. Finally, this induction of MMP-9 facilitates BTB restructuring during the seminiferous epithelial cycle of spermatogenesis. Note that the activation of ERK1/2 after rpS6 phosphorylation might also result in TSC1–TSC2 inhibition and phosphorylation of raptor, thereby enhancing the activity of mTORC1, forming a positive-feedback mechanism. Dotted lines in this figure indicate that other signaling molecules are possibly involved in a yet-to-be-defined mechanism.

Journal of Cell Science (2014) 127, 4870–4882 doi:10.1242/jcs.152231

protein synthesis while mTORC2 controls cell survival and actin remodeling, accumulating evidence has shown that mTORC1 signaling is also involved in mTORC2-mediated cellular functions, such as actin reorganization. For instance, S6Ks were shown to regulate F-actin organization by the activation of the small GTPase Rac1 and Cdc42 (Ip et al., 2011), whereas a delay in actin repolarization after glucose starvation has been demonstrated in yeast after TORC1 inhibition (Aronova et al., 2007). These studies thus demonstrate the interplay between the two mTOR signaling complexes to regulate multiple cellular functions through common upstream signaling pathways. In fact, antagonistic effects of these two signaling complexes have been shown in regulating BTB dynamics, whereby mTORC1 promotes BTB restructuring, whereas mTORC2 confers BTB integrity (Mok et al., 2013b; Mok et al., 2012). Furthermore, another interesting finding in this study is the induction of p-S6Ks and p-4E-BP1 following the overexpression of active rpS6, suggesting that rpS6 phosphorylation might enhance mTORC1 activity, thus creating a positive-feedback loop of mTORC1 signaling. Although the mechanism remains unknown, we propose that the induced mTORC1 activity is triggered by an induction of p-Erk1/2 (Fig. 7). This idea is also supported by other published findings that have shown that Erk1/2 promotes mTORC1 activity by phosphorylating raptor, the key component of mTORC1 (Carriere et al., 2011), and by inhibiting TSC1–TSC2, which is an mTORC1 inhibitor (Ma et al., 2005).

Note that Akt, also known as protein kinase B (PKB), has three isoforms, namely Akt1, Akt2 and Akt3, which share similar structural features but are transcribed from different genes (Wickenden and Watson, 2010). Besides its effect on tumor progression, Akt phosphorylation is known to have protective effects against oxidative stress (Seo et al., 2014) or thermal injury (Han et al., 2014). During these types of stress, Akt protects epithelial barrier function by maintaining the levels of tight junction proteins, illustrating its role in tight junction barrier regulation. Interestingly, although phosphorylation of Akt1 at Ser473 and Akt2 at Ser474 are both dependent on mTORC2 (Dillon and Muller, 2010), studies have shown that Akt1 and Akt2 play different physiological roles in mammalian cells. For instance, although both Akt1 and Akt2 have been shown to regulate palladin, Akt1 regulates its phosphorylation (Chin and Toker, 2010a), whereas Akt2 controls its expression (Chin and Toker, 2010b), illustrating that these two isoforms of Akt1 can have differential effects on a common substrate. Furthermore, light-induced actin reorganization in rod photoreceptor cells is dependent on Akt1 only (Li et al., 2008), whereas plasmin-triggered chemotaxis of dendritic cells is an Akt2-dependent event (Li et al., 2010). Thus, further studies are necessary to define whether these proteins regulate BTB restructuring by different means or different effectors downstream, or whether one is more important than the other in regulating BTB dynamics. Nonetheless, we have demonstrated unequivocally that rpS6, a downstream signaling molecule of mTORC1, regulates BTB dynamics through the insulin/IGF-1 receptor signaling complex upstream, involving PI3-K–PDK1–Akt signaling as well as Erk1/2, which, in turn, modulates MMP-9 expression and activation downstream (Fig. 7). These findings are likely to be applicable to the regulation of other blood–tissue barriers. Additionally, these findings also provide some potential targets for the development of male contraceptives, which could function by perturbing the PI3-K–PDK1–Akt–Erk1/2 signaling pathway through the use of small molecule inhibitors, antagonists and/or agonists.

MATERIALS AND METHODS

Animals

Sprague-Dawley rats were purchased from Charles River Laboratories (Kingston, NY). The use of rats for studies reported herein was approved by the Rockefeller University Institutional Animal Care and Use Committee (IACUC) with Protocol Numbers 09016 and 12506.

Construction of wild-type rpS6 and rpS6 quadruple phosphomimetic mutant and their cloning into mammalian expression vectors

To generate the wild-type rpS6 construct, the full-length coding sequence of wild-type rat ribosomal protein S6 (rpS6; GenBank Accession Number NM_017160.1), including start and stop codons, was amplified from rat Sertoli cell cDNA by PCR using primers listed in supplementary material Table S2, and it was cloned into the *Mlu*I-*Xba*I site of the pCI-neo mammalian expression vector (Promega). This full-length cDNA clone was confirmed by direct nucleotide sequence analysis. To generate the rpS6 quadruple phosphomimetic mutant, i.e. constitutively active rpS6 construct, mutation of rpS6 at residues Ser235, Ser236, Ser240 and Ser244 to glutamic acids was performed by site-directed mutagenesis using PCR with primers containing the desired mutations (supplementary material Table S2) using an approach as described previously (Lie et al., 2012), and the wild-type construct was used as the template. PCR products containing the full-length rpS6 with the desired mutations were then cloned into the pCI-neo vector as mentioned above. All sequences, including all mutation sites, were verified by direct DNA sequencing at Genewiz. For transfection into Sertoli cells, plasmid DNA was prepared with a HiSpeed Plasmid Midi Kit (Qiagen). For the visualization of transfected cells during fluorescent staining, plasmid DNA was labeled with Cy3 using a *Label*IT Tracker Intracellular Nucleic Acid Localization Kit (Mirus).

Primary Sertoli cell cultures, inhibitor treatments, overexpression of rpS6 constructs and knockdowns

Sertoli cells were isolated from testes of 20-day-old rats as described previously (Mruk and Cheng, 2011). Sertoli cells were seeded on Matrigel-coated culture plates (for cell lysate preparation), coverslips (for fluorescence microscopy), Millicell HA 12-mm culture inserts (Millipore) [for transepithelial electrical resistance (TER) measurement to quantify tight junction permeability barrier function] at a density 0.5, 0.05 and 1×10^6 cells/cm^2, respectively. Matrigel was obtained from BD Biosciences and was diluted 1:5–1:7 in medium. Sertoli cells were cultured in a CO_2 incubator in serum-free F12-DMEM (Ham's F12 Nutrient Mixture-Dulbecco's Modified Eagle's Medium; Sigma-Aldrich) supplemented with growth factors, bacitracin and gentamicin as described previously (Mruk and Cheng, 2011) in a humidified atmosphere of 95% air and 5% CO_2 (v/v) at 35℃. Sertoli cells were cultured for 2 days to allow the assembly of a functional tight junction permeability barrier, and the presence of tight junctions, basal ectoplasmic specializations, gap junctions and desmosomes in these cultures was confirmed by electron microscopy as described previously (Lie et al., 2010; Siu et al., 2005). For inhibitor treatments, MMP-9 inhibitor I (a specific inhibitor of MMP-9, EMD Biosciences) or U0126 (a specific inhibitor of Erk1/2, EMD Biosciences) were added to the Sertoli cells at a final concentration of 5 µM and 50 µM, respectively, on day 2, along with the transfection mixture for overexpression for 18 h. Thereafter, inhibitors were included in the complete medium, and the cells were fed daily either until they were harvested on day 4 or TER measurement had finished. LY294002 (a specific inhibitor of PI3-K; Cell Signaling Technology) was added to the Sertoli cells at a final concentration of 50 µM on day 3, along with the transfection mixture for rpS6 knockdown by RNAi. Thereafter, the inhibitor was also included in the complete medium (which was replaced daily) on day 4 until cells were harvested for lysate preparation on day 5. The selection of these concentrations was based on published reports regarding their use in mammalian cells in similar studies involving MMP-9 inhibitor 1 (Adiseshaiah et al., 2008), U0126 (Andrieux et al., 2004) and LY294002 (Guo et al., 2013) without cytotoxicity. For overexpression

Journal of Cell Science (2014) 127, 4870–4882 doi:10.1242/jcs.152231

of empty vector, wild-type rpS6 or active rpS6, Sertoli cells were transfected with the relevant plasmid DNA (~0.45 µg of DNA per 10^6 Sertoli cells) for 18 h using 15 µl of Effectene Transfection Reagent (Qiagen) per microgram of DNA, according to the manufacturer's instructions (Lie et al., 2012). In pilot experiments, luciferase reporter gene activity was assayed as described previously (Xia et al., 2006) to estimate the transfection efficiency for Sertoli cells transfected with luciferase reporter plasmids (pGL3-Control and pRL-TK; Promega). In these experiments, different amounts of plasmid DNA (~0.1–3 µg) and different cell densities ($0.1–1.2\times10^6$ cells/cm^2) were investigated. Cells were transfected for 18–24 h with Effectene Transfection Reagent, and the transfection efficiency was estimated to be ~35%. A transfection efficiency of ~15% was obtained using calcium phosphate for transfection for 4 h. The desired transgenes were maintained for at least 4 days after transfection based on the luciferase assay. Furthermore, successful overexpression of plasmid DNA in Sertoli cells was monitored by using Cy3-labeled DNA, in which plasmid DNA was labeled with Cy3 using a *Label*IT Tracker Intracellular Nucleic Acid Localization Kit (Mirus). For the knockdown experiments, siRNA duplexes targeting Akt1, Akt2 and rpS6 were used, along with non-targeting control siRNA duplexes. Sertoli cells were transfected on day 3 using RiboJuice siRNA transfection reagent (Novagen, EMD Bioscience) for 24 h as described previously (Mok et al., 2013b). Thereafter, cells were washed twice with fresh F12-DMEM. siRNA duplexes were used at 100 nM for transfection of Sertoli cell cultures intended for lysate preparation and fluorescence microscopy; whereas siRNA was used at 200 nM for cultures that were used to assess the tight junction permeability barrier function. The sequences of siRNA duplexes were as follows: Akt1, 5′-CCAGGUAUUUUGAUGAGGAtt-3′ (s127430; Ambion); Akt2, 5′-GGUAUAAAGAGAGACCUGAtt-3′ (s129224; Ambion); rpS6, 5′-GCAGAAUAUGCUAAACUUUtt-3′ (s131129; Ambion). rpS6 RNAi using specific siRNA duplexes was performed as described previously (Mok et al., 2012). Non-targeting siRNA duplex (Silencer Select Negative Control 1 siRNA; Ambion) served as the negative control. Successful transfection using siRNA duplexes were monitored by co-transfecting Sertoli cells with siGLO (Mirus) to assess transfection efficacy. Cells were harvested at 2 days after transfection of plasmid DNA or siRNA duplexes for fluorescence microscopy and preparation of lysates. TER was measured once or twice daily throughout the period of culture as described previously (Mok et al., 2012).

Lysate preparation and immunoblotting

Lysate was prepared from Sertoli cells using immunoprecipitation lysis buffer [50 mM Tris pH 7.4 at 22℃, containing 0.15 M NaCl, 1% Nonidet P-40 (v/v), 1 mM EGTA, 2 mM N-ethylmaleimide, 10% glycerol (v/v)] supplemented with protease inhibitor mixture (Sigma-Aldrich) and phosphatase inhibitor mixture II and III (Sigma-Aldrich) at a dilution of 1:66.7 as specified by the manufacturer. Protein concentration was estimated using a BioRad D_c Protein Assay kit with a BioRad Model 680 Spectrophotometry Reader using BSA as a standard. Unless otherwise specified, ~35 µg of protein from lysate was used per lane for immunoblotting as described previously (Mok et al., 2013b). Antibodies used for immunoblot analysis, dual-labeled immunofluorescence and immunohistochemistry and the appropriate dilutions are listed in supplementary material Table S1.

PI3-K activity assay

Sertoli cell lysates were prepared from cells transfected with different plasmid DNAs using immunoprecipitation lysis buffer supplemented with protease inhibitor mixture and phosphatase inhibitor mixtures II and III as described above. After diluting the lysate from different samples to the same protein concentration, lysates were subjected to immunoprecipitation of PI3-K using a specific anti-PI3-K antibody (supplementary material Table S1). Lysate was pre-cleared prior to immunoprecipitation as described previously (Lie et al., 2012; Mok et al., 2012), followed by incubation with anti-PI3-K antibody for 2 h at 4℃, and then incubation with 40 µl of Protein A/G Plus overnight at 4℃ to precipitate the immunocomplexes. After spinning at 1000 ***g*** (5 min at 4°C) to collect the immunocomplex/PI3-K-containing Protein A/G Plus by discarding the lysates, Protein A/G Plus was washed twice. Thereafter, the immunocomplex/PI3-K-containing Protein A/G Plus was subjected to a PI3-K activity assay using the PI3-Kinase Activity ELISA: Pico assay kit (Echelon Biosciences) according to the manufacturer's protocol. Briefly, PIP_3 was first generated by incubating the PI3-K-containing Protein A/G Plus beads with PIP_2 solution for 3 h at 37℃. Reactions were stopped and, after spinning down the Protein A/G Plus, supernatants were collected and incubated with PIP_3 detector for 1 h at room temperature with gentle agitation. Thereafter, reaction mixtures were transferred to the detection plate with wells coated with PIP_3 (which competed for PIP_3 detector with the PIP_3 generated from the former reaction) and were incubated for 1 h at room temperature with gentle agitation. Reaction mixtures were then discarded, and the wells were washed with TBS-T (50 mM Tris-HCl pH 7.4, 150 mM NaCl, 0.05% Tween 20, at 22℃). The supplied secondary detector was added to the detection plate and the reactions were incubated for 30 min at room temperature with gentle agitation. Solutions were then discarded and wells were washed with TBS-T. Thereafter, the supplied TMB solution was added to the detection plate for color development. Note that the more PIP_3 generated during the incubation of immunocomplexes containing Protein A/G Plus beads, the less the PIP_3 detector would be available for binding to the detection plate. Therefore, the intensity of the color developed is inversely proportional to the activity of PI3-K in the lysates. Reactions were then stopped by the addition of 0.5 M H_2SO_4 until the color turned dark blue in the buffer-alone control well. The plate was then read by using a BioRad Model 680 Spectrophotometry Reader at absorbance 480 nm.

Dual-labeled immunofluorescence analysis and quantification of immunofluorescent signal intensity of tight junction proteins at the cell–cell interface

Bouin's-fixed testes were embedded in paraffin, sectioned to 5 µm with a microtome and mounted on positively charged glass microscopic slides. Before permeabilization of sections of testes with Triton X-100 as mentioned later on, antigen retrieval was performed by boiling paraffin sections on slides in Tris-EDTA buffer [10 mM Tris pH 9.0 at 22℃, containing 1 mM EDTA and 0.05% Tween (v/v)] for 20 min. Paraffin sections were only used for staining p-Akt1-Ser473 or p-Akt2-Ser474. Frozen sections of testes (7 µm in thickness), obtained with a cryostat at −22℃ and mounted on poly-L-lysine-coated slides (Polysciences), or Sertoli cells cultured on Matrigel-coated coverslips at a density 0.05×10^6 cells/cm^2 were fixed in 4% paraformaldehyde in PBS (10 mM sodium phosphate, 0.15 M NaCl, pH 7.4 at 22℃) (w/v) for 10 min and were permeabilized in 0.1% Triton X-100 in PBS (v/v) for 4 min. Sections or cells were then blocked in 1% BSA in PBS (w/v) (blocking solution) for 30 min, followed by an overnight incubation with primary antibodies (supplementary material Table S1) diluted in blocking solution at room temperature. Thereafter, sections or cells were incubated with Alexa-Fluor-conjugated secondary antibodies (Invitrogen; red fluorescence, Alexa Fluor 555; green fluorescence, Alexa Fluor 488) at 1:250 dilution with blocking solution at room temperature for 1 hour. Sections or cells were mounted with Prolong Gold antifade mounting medium with DAPI (Invitrogen). Fluorescence images were captured using a Nikon Eclipse 90i Fluorescence Microscope with a Nikon DS-Qi1Mc digital camera, acquired using Nikon NIS Elements Imaging Software (Version 3.2) (Nikon Instruments, Melville, NY). Brightness and contrast adjustments and image overlay were performed in Photoshop using the Adobe Creative Suite (Version 3.0) software package. All experiments, including dual-labeled immunofluorescence analysis and immunohistochemistry, were repeated at least three times using testes from different rats or different preparations of Sertoli cell cultures. All samples (sections of testes or Sertoli cells) within an experimental group were processed simultaneously in a single experimental session to eliminate inter-experimental variations. To compare immunofluorescent signals at the cell–cell interface in both treatment and control groups, the fluorescence intensity in treated and control cells was quantified by using the software ImageJ as described previously (Mok et al., 2012). Fluorescent signals of tight junction proteins at the Sertoli cell–cell interface of ~50 randomly

selected cells from an experiment (with a total of three independent experiments) were quantified.

MMP-9 activity assay

After Sertoli cells were transfected with different plasmid DNAs on day 2, medium from the rpS6 mutant versus wild-type rpS6 and control (empty vector) group was collected on day 4 and concentrated using EMD Millipore Ultracel 10K filters (4000 ***g*** for 20 min at 4℃). Concentrated medium was diluted to equal volumes for all samples, and the amount of MMP-9 in each sample was quantified by using the MMP-9 assay kit (AnaSpec). Briefly, medium prepared as above was added to the wells of an ELISA plate coated with anti-MMP-9 antibody, followed by incubation for 1 h with gentle agitation. The medium was then discarded and, after washing the wells with the washing buffer, 1 mM APMA (4-aminophenyl mercuric acetate, for activating the pro-MMP-9) was added and the reaction was incubated at room temperature for 2 h with gentle agitation. AMPA solution was then discarded and, after washing the wells, MMP-9 substrate solution was added and the proteolytic cleavage reaction was performed at room temperature in the dark for 16 h. When MMP-9 reacted with the substrate, an increase in fluorescence emission at 508–548 nm was detected. Readings were taken (top reading) at room temperature with a FilterMax F5 Multi-Mode Microplate Reader (Molecular Devices) using a Multi-Mode Analysis Software Package (Version 3.4; Molecular Devices).

Statistical analysis

All data presented in the figures in this report are representative findings of an experiment except for bar graphs, which are composite data of $n=4$–6 independent experiments. These experiments were repeated 4–6 times using different batches of Sertoli cells that yielded similar results. Statistical analysis was performed using the GB-STAT software package (Version 7.0; Dynamic Microsystems) to carry out two-way ANOVA followed by Newman-Keul's test.

Competing interests

The authors declare no competing interests.

Author contributions

C.Y.C. conceived of the project. K.-W.M. and C.Y.C. designed and performed the experiments, and analyzed the data. K.-W.M., D.D.M. and C.Y.C. evaluated data and interpreted the findings. K.-W.M. and C.Y.C. wrote the paper.

Funding

This work was supported in part by grants from the National Institutes of Health (National Institute of Child Health and Human Development) [grant numbers R01 HD056034 and U54 HD029990 Project 5 to C.Y.C.]. Deposited in PMC for release after 12 months.

Supplementary material

Supplementary material available online at
http://jcs.biologists.org/lookup/suppl/doi:10.1242/jcs.152231/-/DC1

References

Adiseshaiah, P., Vaz, M., Machireddy, N., Kalvakolanu, D. V. and Reddy, S. P. (2008). A Fra-1-dependent, matrix metalloproteinase driven EGFR activation promotes human lung epithelial cell motility and invasion. *J. Cell. Physiol.* **216**, 405-412.

Andrieux, L., Langouët, S., Fautrel, A., Ezan, F., Krauser, J. A., Savouret, J. F., Guengerich, F. P., Baffet, G. and Guillouzo, A. (2004). Aryl hydrocarbon receptor activation and cytochrome P450 1A induction by the mitogen-activated protein kinase inhibitor U0126 in hepatocytes. *Mol. Pharmacol.* **65**, 934-943.

Aronova, S., Wedaman, K., Anderson, S., Yates, J., III and Powers, T. (2007). Probing the membrane environment of the TOR kinases reveals functional interactions between TORC1, actin, and membrane trafficking in Saccharomyces cerevisiae. *Mol. Biol. Cell* **18**, 2779-2794.

Björklund, M. and Koivunen, E. (2005). Gelatinase-mediated migration and invasion of cancer cells. *Biochim. Biophys. Acta* **1755**, 37-69.

Carriere, A., Romeo, Y., Acosta-Jaquez, H. A., Moreau, J., Bonneil, E., Thibault, P., Fingar, D. C. and Roux, P. P. (2011). ERK1/2 phosphorylate Raptor to promote Ras-dependent activation of mTOR complex 1 (mTORC1). *J. Biol. Chem.* **286**, 567-577.

Chen, F., Ohashi, N., Li, W., Eckman, C. and Nguyen, J. H. (2009). Disruptions of occludin and claudin-5 in brain endothelial cells in vitro and in brains of mice with acute liver failure. *Hepatology* **50**, 1914-1923.

Chen, F., Radisky, E. S., Das, P., Batra, J., Hata, T., Hori, T., Baine, A. M., Gardner, L., Yue, M. Y., Bu, G. et al. (2013). TIMP-1 attenuates blood-brain barrier permeability in mice with acute liver failure. *J. Cereb. Blood Flow Metab.* **33**, 1041-1049.

Cheng, C. Y. and Mruk, D. D. (2010). A local autocrine axis in the testes that regulates spermatogenesis. *Nat. Rev. Endocrinol.* **6**, 380-395.

Cheng, C. Y. and Mruk, D. D. (2012). The blood-testis barrier and its implications for male contraception. *Pharmacol. Rev.* **64**, 16-64.

Chin, Y. R. and Toker, A. (2010a). The actin-bundling protein palladin is an Akt1-specific substrate that regulates breast cancer cell migration. *Mol. Cell* **38**, 333-344.

Chin, Y. R. and Toker, A. (2010b). Akt2 regulates expression of the actin-bundling protein palladin. *FEBS Lett.* **584**, 4769-4774.

Chiu, P. S. and Lai, S. C. (2013). Matrix metalloproteinase-9 leads to claudin-5 degradation via the NF-κB pathway in BALB/c mice with eosinophilic meningoencephalitis caused by Angiostrongylus cantonensis. *PLoS ONE* **8**, e53370.

Copp, J., Manning, G. and Hunter, T. (2009). TORC-specific phosphorylation of mammalian target of rapamycin (mTOR): phospho-Ser2481 is a marker for intact mTOR signaling complex 2. *Cancer Res.* **69**, 1821-1827.

Das, G., Shiras, A., Shanmuganandam, K. and Shastry, P. (2011). Rictor regulates MMP-9 activity and invasion through Raf-1-MEK-ERK signaling pathway in glioma cells. *Mol. Carcinog.* **50**, 412-423.

Dillon, R. L. and Muller, W. J. (2010). Distinct biological roles for the akt family in mammary tumor progression. *Cancer Res.* **70**, 4260-4264.

Fayard, E., Xue, G., Parcellier, A., Bozulic, L. and Hemmings, B. A. (2010). Protein kinase B (PKB/Akt), a key mediator of the PI3K signaling pathway. *Curr. Top. Microbiol. Immunol.* **346**, 31-56.

Guo, Y., Chen, Y., Liu, L. B., Chang, K. K., Li, H., Li, M. Q. and Shao, J. (2013). IL-22 in the endometriotic milieu promotes the proliferation of endometrial stromal cells via stimulating the secretion of CCL2 and IL-8. *Int. J. Clin. Exp. Pathol.* **6**, 2011-2020.

Han, J. T., Zhang, W. F., Wang, Y. C., Cai, W. X., Lv, G. F. and Hu, D. H. (2014). Insulin protects against damage to pulmonary endothelial tight junctions after thermal injury: relationship with zonula occludens-1, F-actin, and AKT activity. *Wound Repair Regen.* **22**, 77-84.

Harrington, L. S., Findlay, G. M., Gray, A., Tolkacheva, T., Wigfield, S., Rebholz, H., Barnett, J., Leslie, N. R., Cheng, S., Shepherd, P. R. et al. (2004). The TSC1-2 tumor suppressor controls insulin-PI3K signaling via regulation of IRS proteins. *J. Cell Biol.* **166**, 213-223.

Ip, C. K., Cheung, A. N., Ngan, H. Y. and Wong, A. S. (2011). p70 S6 kinase in the control of actin cytoskeleton dynamics and directed migration of ovarian cancer cells. *Oncogene* **30**, 2420-2432.

Janecki, A., Jakubowiak, A. and Steinberger, A. (1992). Effect of cadmium chloride on transepithelial electrical resistance of Sertoli cell monolayers in two-compartment cultures—a new model for toxicological investigations of the ''blood-testis'' barrier in vitro. *Toxicol. Appl. Pharmacol.* **112**, 51-57.

Laplante, M. and Sabatini, D. M. (2012). mTOR signaling in growth control and disease. *Cell* **149**, 274-293.

Lee, N. P. Y. and Cheng, C. Y. (2003). Regulation of Sertoli cell tight junction dynamics in the rat testis via the nitric oxide synthase/soluble guanylate cyclase/3′,5′-cyclic guanosine monophosphate/protein kinase G signaling pathway: an in vitro study. *Endocrinology* **144**, 3114-3129.

Li, G., Rajala, A., Wiechmann, A. F., Anderson, R. E. and Rajala, R. V. (2008). Activation and membrane binding of retinal protein kinase Balpha/Akt1 is regulated through light-dependent generation of phosphoinositides. *J. Neurochem.* **107**, 1382-1397.

Li, X., Syrovets, T., Genze, F., Pitterle, K., Oberhuber, A., Orend, K. H. and Simmet, T. (2010). Plasmin triggers chemotaxis of monocyte-derived dendritic cells through an Akt2-dependent pathway and promotes a T-helper type-1 response. *Arterioscler. Thromb. Vasc. Biol.* **30**, 582-590.

Lie, P. P. Y., Cheng, C. Y. and Mruk, D. D. (2010). Crosstalk between desmoglein-2/desmocollin-2/Src kinase and coxsackie and adenovirus receptor/ZO-1 protein complexes, regulates blood-testis barrier dynamics. *Int. J. Biochem. Cell Biol.* **42**, 975-986.

Lie, P. P., Mruk, D. D., Mok, K. W., Su, L., Lee, W. M. and Cheng, C. Y. (2012). Focal adhesion kinase-Tyr407 and -Tyr397 exhibit antagonistic effects on blood-testis barrier dynamics in the rat. *Proc. Natl. Acad. Sci. USA* **109**, 12562-12567.

Longin, J., Guillaumot, P., Chauvin, M. A., Morera, A. M., Le Magueresse-Battistoni, B. (2001) MT1-MMP in rat testicular development and the control of Sertoli cell proMMP-2 activation. *J. Cell Sci.* **124**, 2125-2134.

Lui, W. Y., Wong, C. H., Mruk, D. D. and Cheng, C. Y. (2003). TGF-β3 regulates the blood-testis barrier dynamics via the p38 mitogen activated protein (MAP) kinase pathway: an in vivo study. *Endocrinology* **144**, 1139-1142.

Ma, L., Chen, Z., Erdjument-Bromage, H., Tempst, P. and Pandolfi, P. P. (2005). Phosphorylation and functional inactivation of TSC2 by Erk implications for tuberous sclerosis and cancer pathogenesis. *Cell* **121**, 179-193.

Masure, S., Haefner, B., Wesselink, J. J., Hoefnagel, E., Mortier, E., Verhasselt, P., Tuytelaars, A., Gordon, R. and Richardson, A. (1999). Molecular cloning, expression and characterization of the human serine/threonine kinase Akt-3. *Eur. J. Biochem.* **265**, 353-360.

Meyuhas, O. (2008). Physiological roles of ribosomal protein S6: one of its kind. *Int. Rev. Cell Mol. Biol.* **268**, 1-37.

Moelling, K., Schad, K., Bosse, M., Zimmermann, S. and Schweneker, M. (2002). Regulation of Raf-Akt Cross-talk. *J. Biol. Chem.* **277**, 31099-31106.
Mok, K. W., Mruk, D. D., Silvestrini, B. and Cheng, C. Y. (2012). rpS6 Regulates blood-testis barrier dynamics by affecting F-actin organization and protein recruitment. *Endocrinology* **153**, 5036-5048.
Mok, K. W., Mruk, D. D. and Cheng, C. Y. (2013a). Regulation of blood-testis barrier (BTB) dynamics during spermatogenesis via the ''Yin'' and ''Yang'' effects of mammalian target of rapamycin complex 1 (mTORC1) and mTORC2. *Int. Rev. Cell Mol. Biol.* **301**, 291-358.
Mok, K. W., Mruk, D. D., Lee, W. M. and Cheng, C. Y. (2013b). Rictor/mTORC2 regulates blood-testis barrier dynamics via its effects on gap junction communications and actin filament network. *FASEB J.* **27**, 1137-1152.
Mruk, D. D. and Cheng, C. Y. (2011). An in vitro system to study Sertoli cell blood-testis barrier dynamics. *Methods Mol. Biol.* **763**, 237-252.
Mruk, D. D., Silvestrini, B. and Cheng, C. Y. (2008). Anchoring junctions as drug targets: role in contraceptive development. *Pharmacol. Rev.* **60**, 146-180.
Nicholls, P. K., Harrison, C. A., Gilchrist, R. B., Farnworth, P. G. and Stanton, P. G. (2009). Growth differentiation factor 9 is a germ cell regulator of Sertoli cell function. *Endocrinology* **150**, 2481-2490.
Oh, W. J. and Jacinto, E. (2011). mTOR complex 2 signaling and functions. *Cell Cycle* **10**, 2305-2316.
Petecchia, L., Sabatini, F., Usai, C., Caci, E., Varesio, L. and Rossi, G. A. (2012). Cytokines induce tight junction disassembly in airway cells via an EGFR-dependent MAPK/ERK1/2-pathway. *Lab. Invest.* **92**, 1140-1148.
Qiu, L., Zhang, X., Zhang, X., Zhang, Y., Gu, J., Chen, M., Zhang, Z., Wang, X. and Wang, S. L. (2013). Sertoli cell is a potential target for perfluorooctane sulfonate-induced reproductive dysfunction in male mice. *Toxicol. Sci.* **135**, 229-240.
Roux, P. P., Ballif, B. A., Anjum, R., Gygi, S. P. and Blenis, J. (2004). Tumor-promoting phorbol esters and activated Ras inactivate the tuberous sclerosis tumor suppressor complex via p90 ribosomal S6 kinase. *Proc. Natl. Acad. Sci. USA* **101**, 13489-13494.
Russell, L. (1977). Movement of spermatocytes from the basal to the adluminal compartment of the rat testis. *Am. J. Anat.* **148**, 313-328.
Samak, G., Aggarwal, S. and Rao, R. K. (2011). ERK is involved in EGF-mediated protection of tight junctions, but not adherens junctions, in acetaldehyde-treated Caco-2 cell monolayers. *Am. J. Physiol.* **301**, G50-G59.
Sarbassov, D. D., Guertin, D. A., Ali, S. M. and Sabatini, D. M. (2005). Phosphorylation and regulation of Akt/PKB by the rictor-mTOR complex. *Science* **307**, 1098-1101.
Seo, G. S., Jiang, W. Y., Park, P. H., Sohn, D. H., Cheon, J. H. and Lee, S. H. (2014). Hirsutenone reduces deterioration of tight junction proteins through EGFR/Akt and ERK1/2 pathway both converging to HO-1 induction. *Biochem. Pharmacol.* **90**, 115-125.
Shah, O. J., Anthony, J. C., Kimball, S. R. and Jefferson, L. S. (2000). 4E-BP1 and S6K1: translational integration sites for nutritional and hormonal information in muscle. *Am. J. Physiol.* **279**, E715-E729.
Siu, M. K. Y. and Cheng, C. Y. (2004) Interactions of proteases, protease inhibitors, and the beta1 integrin/laminin gamma3 protein complex in the regulation of ectoplasmic specialization dynamics in the rat testis. *Biol. Reprod.* **70**, 945-964.
Siu, M. K. Y., Wong, C. H., Lee, W. M. and Cheng, C. Y. (2005). Sertoli-germ cell anchoring junction dynamics in the testis are regulated by an interplay of lipid and protein kinases. *J. Biol. Chem.* **280**, 25029-25047.
Smith, B. E. and Braun, R. E. (2012). Germ cell migration across Sertoli cell tight junctions. *Science* **338**, 798-802.
Song, G., Ouyang, G. and Bao, S. (2005). The activation of Akt/PKB signaling pathway and cell survival. *J. Cell. Mol. Med.* **9**, 59-71.
Su, L., Mruk, D. D., Lie, P. P. Y., Silvestrini, B. and Cheng, C. Y. (2012). A peptide derived from laminin-γ3 reversibly impairs spermatogenesis in rats. *Nat. Commun.* **3**, 1185.
Thorburn, A. (2004). Death receptor-induced cell killing. *Cell. Signal.* **16**, 139-144.
Tseng, H. C., Lee, I. T., Lin, C. C., Chi, P. L., Cheng, S. E., Shih, R. H., Hsiao, L. D. and Yang, C. M. (2013). IL-1β promotes corneal epithelial cell migration by increasing MMP-9 expression through NF-κB- and AP-1-dependent pathways. *PLoS ONE* **8**, e57955.
Tsokas, P., Ma, T., Iyengar, R., Landau, E. M. and Blitzer, R. D. (2007). Mitogen-activated protein kinase upregulates the dendritic translation machinery in long-term potentiation by controlling the mammalian target of rapamycin pathway. *J. Neurosci.* **27**, 5885-5894.
Tyagi, N., Gillespie, W., Vacek, J. C., Sen, U., Tyagi, S. C. and Lominadze, D. (2009). Activation of GABA-A receptor ameliorates homocysteine-induced MMP-9 activation by ERK pathway. *J. Cell Physiol.* **220**, 257-266.
Vallejo, A. N., Pogulis, R. J. and Pease, L. R. (2008). PCR mutagenesis by overlap extension and gene SOE. *Cold Spring Harb. Protoc.* **2008**, pdb.prot4861.
Wan, H. T., Mruk, D. D., Li, S. Y. T., Mok, K. W., Lee, W. M., Wong, C. K. C. and Cheng, C. Y. (2013). p-FAK-Tyr(^{397}) regulates spermatid adhesion in the rat testis via its effects on F-actin organization at the ectoplasmic specialization. *Am. J. Physiol.* **305**, E687-E699.
Weichhart, T. (2012). Mammalian target of rapamycin: a signaling kinase for every aspect of cellular life. *Methods Mol. Biol.* **821**, 1-14.
Wickenden, J. A. and Watson, C. J. (2010). Key signalling nodes in mammary gland development and cancer. Signalling downstream of PI3 kinase in mammary epithelium: a play in 3 Akts. *Breast Cancer Res.* **12**, 202.
Xia, W., Mruk, D. D., Lee, W. M. and Cheng, C. Y. (2006). Differential interactions between transforming growth factor-β3/TbetaR1, TAB1, and CD2AP disrupt blood-testis barrier and Sertoli-germ cell adhesion. *J. Biol. Chem.* **281**, 16799-16813.
Zhang, H., Cicchetti, G., Onda, H., Koon, H. B., Asrican, K., Bajraszewski, N., Vazquez, F., Carpenter, C. L. and Kwiatkowski, D. J. (2003). Loss of Tsc1/Tsc2 activates mTOR and disrupts PI3K-Akt signaling through downregulation of PDGFR. *J. Clin. Invest.* **112**, 1223-1233.
Zimmermann, S. and Moelling, K. (1999). Phosphorylation and regulation of Raf by Akt (protein kinase B). *Science* **286**, 1741-1744.